

Low-temperature properties of the dilute dipolar magnet $\text{LiHo}_x\text{Y}_{1-x}\text{F}_4$

A. Biltmo and P. Henelius

Department of Theoretical Physics, Royal Institute of Technology, SE-106 91 Stockholm, Sweden

(Received 6 March 2008; revised manuscript received 15 May 2008; published 25 August 2008)

We analyze recent experiments on the dilute rare-earth compound $\text{LiHo}_x\text{Y}_{1-x}\text{F}_4$ in the context of an effective Ising dipolar model. Using a Monte Carlo method we calculate the low-temperature behavior of the specific heat and linear susceptibility and compare our results to measurements. In our model the susceptibility follows a Curie-Weiss law at high temperature, $\chi \sim 1/(T - T_{\text{cw}})$, with a Curie-Weiss temperature that scales with dilution, $T_{\text{cw}} \sim x$, consistent with early experiments. We also find that the peak in the specific heat scales linearly with dilution, $C_{\text{max}}(T) \sim x$, in disagreement with recent experiments. This difference could be caused by the hyperfine interaction which is not included in our calculation. Experimental studies do not reach a consensus on the functional form of the susceptibility and specific heat, and in particular, we do not see reported scalings of the form $\chi \sim T^{-0.75}$ and $\chi \sim \exp(-T/T_0)$. Furthermore, we calculate the ground-state magnetization as a function of dilution and re-examine the phase diagram around the critical dilution $x_c = 0.24 \pm 0.03$. We find that the spin-glass susceptibility for the Ising model does not diverge below x_c , while some recent experiments give strong evidence for a stable spin-glass phase in $\text{LiHo}_{0.167}\text{Y}_{0.833}\text{F}_4$.

DOI: [10.1103/PhysRevB.78.054437](https://doi.org/10.1103/PhysRevB.78.054437)

PACS number(s): 75.10.Hk, 75.50.Lk, 75.40.Mg

I. INTRODUCTION

The rare-earth compound LiHoF_4 is used as a model magnet to investigate diverse magnetic phenomena such as quantum phase transitions,¹ spin-glass behavior,² and quantum annealing.³ The magnetic behavior arises from the Ho^{3+} ions which have tightly bound $4f$ electrons. This causes the exchange interaction to be weak, and the inter-ion interactions are predominantly dipolar. The local crystal field causes a strong anisotropy, and the interaction is Ising-like. To a first approximation LiHoF_4 is therefore believed to be good realization of a dipolar Ising model,⁴

$$H = \frac{J}{2} \sum_{i \neq j} \frac{r_{ij}^2 - 3z_{ij}^2}{r_{ij}^5} \sigma_i^z \sigma_j^z + \frac{J_{\text{ex}}}{2} \sum_{i, \text{nn}} \sigma_i^z \sigma_{\text{nn}}^z, \quad (1)$$

where we have used a dipolar coupling constant $J = 0.214$ K and a nearest-neighbor (nn) exchange coupling $J_{\text{ex}} = 0.12$ K.⁵ The interspin distance is r_{ij} with a component z_{ij} along the Ising axis. The magnetic Ho^{3+} ions sit on a tetragonal lattice with four ions per unit cell. To study quantum criticality a transverse magnetic field can be applied, and in order to study the effects of disorder, the magnetic Ho^{3+} ions can be substituted by nonmagnetic Y^{3+} ions, resulting in $\text{LiHo}_x\text{Y}_{1-x}\text{F}_4$. At low temperatures, or in the limit of high dilution, the single-ion properties such as the hyperfine coupling become important corrections to the above model.

During the past three decades LiHoF_4 has been extensively studied and used as a textbook example of a quantum magnet.^{6,7} However, in the case of substantial dilution experimental studies have reported a variety of functional forms for basic thermodynamic quantities, such as the static susceptibility and the specific heat. The earliest data we find for the static susceptibility report a high-temperature Curie-Weiss scaling $\chi \sim 1/(T - T_{\text{cw}})$ with Curie-Weiss temperatures $T_{\text{cw}} = 0.05$ and 0.16 for dilution $x = 0.045$ and 0.167 , respectively.² In a later work the susceptibility is found to diverge with a different power law, $\chi \sim T^{-0.75}$ ($x = 0.045$),⁸ and in a recent study the exponential low-temperature form

$\chi = \exp(-T/T_0)$ is reported.⁹ The specific heat has also been measured by several different groups, and in an earlier study of the specific heat a peak was found at about $T = 0.3$ K for $x = 0.045$, while there was only a much broader maximum below $T = 0.2$ K for $x = 0.167$.² An extension of these data displays an additional peak at $T = 0.1$ K for $x = 0.045$.⁸ A more recent study¹⁰ displays a dilution independent maximum in the specific heat at about $T = 0.1$ K for $x = 0.018$, 0.045 , and 0.08 .

Finally, the nature of the glassy phase at low temperatures has also been the topic of several experimental studies. Earlier work found a spin-liquid (antiglass) phase at high dilution ($x = 0.045$), followed by a stable spin-glass phase at dilution $x = 0.167$, and finally a magnetic phase at $x = 0.3$.² More recent experiments did not detect a spin-glass transition,⁹ but this may have been due to the use of large magnetic fields,¹¹ a possibility which the authors in Ref. 9 reject.¹² Recent numerical work on dilute dipoles on a small cubic lattice fails to find a spin-glass transition¹³ and so does a recent numerical study of the above model for $\text{LiHo}_x\text{Y}_{1-x}\text{F}_4$.⁵

In this study we confine ourselves to the case of no external magnetic field, but it is interesting to note that quantum Monte Carlo studies of the above nondiluted model including an applied transverse field^{4,14} do not reach quantitative agreement with the experimental phase diagram, even for small transverse fields. Much of the recent theoretical work on $\text{LiHo}_x\text{Y}_{1-x}\text{F}_4$ has focused on the effects of the hyperfine coupling and off-diagonal dipolar terms resulting in corrections to the above Hamiltonian.¹⁵⁻¹⁸ Yet a nonperturbative calculation beyond mean field of several fundamental properties, such as the specific heat and linear susceptibility, is lacking even for the model described by Eq. (1). The goal of the present work is to numerically investigate the above model and determine to what extent it can be used to interpret the experimental results. In particular, we calculate the static susceptibility and specific heat and compare our result to recent experiments. We also calculate the ground-state magnetization as a function of temperature in order to get an

independent estimate of the critical dilution, x_c , where the magnetization vanishes. Finally, we reexamine the low-temperature disordered phase and search for evidence of a stable spin-glass phase.

II. METHOD

We have used a single spin-flip Monte Carlo method and applied periodic boundary conditions. To handle the long-range nature of the interaction we have used the Ewald summation method¹⁹ as explained in an earlier study.⁵ To overcome energy barriers in the glassy phase and reach lower temperatures than in previous work, we have used the replica exchange Monte Carlo method.²⁰ The method involves simulating an ensemble of systems at suitably chosen temperatures T_i , and the algorithm has two main phases. In the first phase each replica is independently evolved in (Monte Carlo) time using the single spin Metropolis algorithm. In the second phase attempts are made to exchange the replicas at adjacent temperatures T_i and T_{i+1} . A full Monte Carlo step consists of one attempted spin flip per spin (on average) followed by ten attempts to exchange neighboring replicas. For the simulation to converge at low temperatures it is important that the swap rate of the replicas is not too low. Theory and empirical studies^{21,22} have shown the optimal rate to be around 20% and these simulations were carried out with swap rates of $\geq 20\%$.

In the present study we have calculated the specific heat,

$$C = \frac{1}{k_B T^2} (\langle H^2 \rangle - \langle H \rangle^2), \quad (2)$$

and the magnetic susceptibility,

$$\chi = \frac{1}{T} (\langle M^2 \rangle - \langle M \rangle^2), \quad (3)$$

where the magnetization $M = \sum_{i=1}^N \sigma_i^z$.

In order to study the disordered phase we have calculated the Edwards-Anderson overlap between two replicas,²³

$$q = \frac{1}{N} \sum_i \sigma_{i,1}^z \sigma_{i,2}^z,$$

and the corresponding Binder ratio,

$$g_q = 1 - \frac{\langle q^4 \rangle}{3 \langle q^2 \rangle^2}.$$

The spin-glass susceptibility is defined as $\chi_{SG} = \langle q^2 \rangle / T^2$. In addition to the thermal average we have calculated an average of 400–600 quenched disorder realizations.

III. RESULTS

First we compare our calculation of the specific heat to experimental data. In Fig. 1 we show experimental data for $x=0.045$ and $x=0.167$ from Refs. 8 and 2, respectively. In the same figure we show our results for $x=0.045$ and $x=0.165$. The data for $x=0.167$ and $x=0.165$ agree qualitatively with both experiment and calculation showing a broad

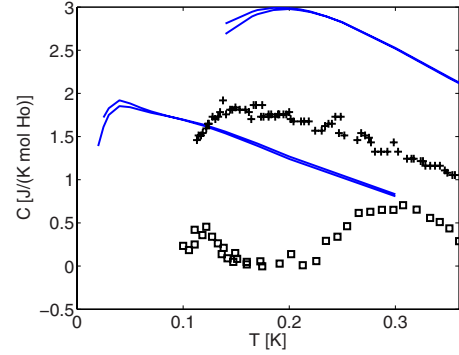


FIG. 1. (Color online) Specific heat as a function of temperature. Experimental data (open symbols) for dilutions $x=0.167$ and $x=0.045$ (top to bottom) from Refs. 8 and 2. Monte Carlo results (solid lines) for dilutions $x=0.165$ and 0.045 (top to bottom). To display the limited finite-size effects results for 8^3 (lower curve) and 10^3 (upper curve) unit cells are shown for dilution $x=0.045$, and 12^3 (lower curve) and 14^3 (upper curve) unit cells for dilution $x=0.165$. Statistical errors are smaller than the finite-size effects.

maximum below $T=0.2$. However, the height of the experimental maximum is about 30% lower than the height of the calculated maximum. The results for $x=0.045$ disagree in a qualitative way since the experimental data features two peaks, one at $T=0.1$ K and the other at $T=0.3$ K, while the calculation yields a peak at about $T=0.05$ K.

In Fig. 2 we show recent experimental data for $x=0.018$ and $x=0.045$ and $x=0.08$ from Ref. 10. Both sets of curves indicate that the specific heat grows with decreasing dilution, and both sets of curves exhibit a maximum for some intermediate temperature. However, the experimental peak position is roughly independent of the dilution, while the calculated peak position scales linearly with x , which can be seen in Fig. 3. In an Ising spin glass the specific heat exhibits a broad maximum in the vicinity of the transition temperature,²³ and as several properties, such as the mean-field transition temperature (see Fig. 3) also scale linearly with dilution, we may expect the calculated behavior for the

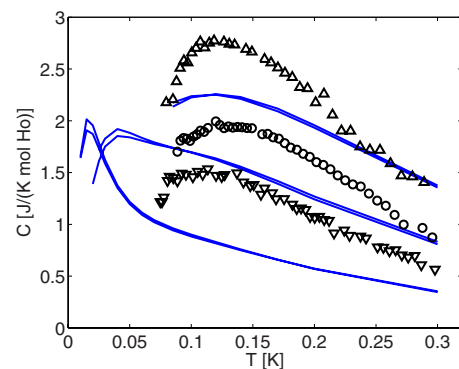


FIG. 2. (Color online) Specific heat as a function of temperature. Experimental data from Ref. 10 (open symbols) for dilutions $x=0.08$, 0.045 , and 0.018 (top to bottom). Monte Carlo results (solid lines) for dilutions $x=0.08$, 0.045 , and 0.018 (top to bottom). To display the limited finite-size effects results for 8^3 (lower curve) and 10^3 (upper curve) unit cells are shown for each dilution. Statistical errors are smaller than the finite-size effects.

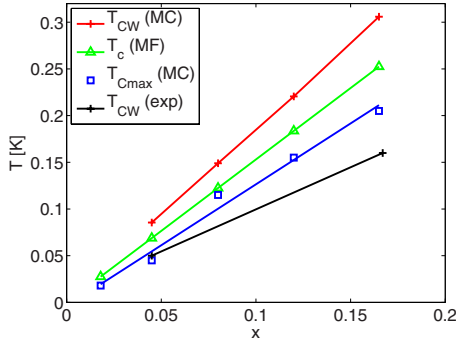


FIG. 3. (Color online) Curie-Weiss temperature (Monte Carlo), mean-field critical temperature, maximum in specific heat (Monte Carlo), and experimental Curie-Weiss temperature from Ref. 2 (top to bottom) as a function of dilution. Statistical errors are the size of the symbols.

model described by Eq. (1). The difference between the experiments and our calculation could be explained by single-ion properties, such as the hyperfine coupling, which become increasingly important in the high-dilution limit but are omitted in the calculation. In fact, for the least dilute systems ($x=0.08$ and 0.167) the calculated and the measured peak position agree quite well. It would be interesting to measure the specific heat also for less dilute systems to see whether the expected linear increase in the peak position of the specific heat is recovered in this limit.

Next we analyze our results for the linear susceptibility. The inverse susceptibility is plotted in Fig. 4. In good qualitative agreement with early measurements of the susceptibility² we see Curie-Weiss behavior, $\chi \sim 1/(T - T_{cw})$, at higher temperatures and deviations at low temperatures. As the dilution is increased the susceptibility approaches the free spin limit $\chi \sim T^{-1}$ as expected. Extrapolating the Curie scaling to the intercept gives us the Curie-Weiss temperature, T_{cw} , which is positive, in accordance with the ferromagnetic correlations in LiHoF₄. As can be seen in Fig. 3 we find that T_{cw} scales linearly in x , and we get $T_{cw}=0.08$ and 0.30 for

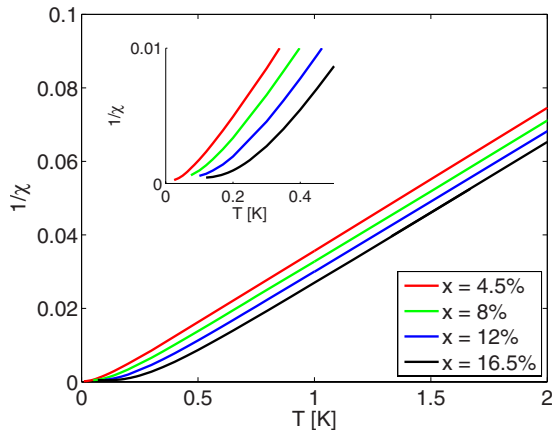


FIG. 4. (Color online) Inverse susceptibility per spin as a function of temperature for $x=0.045, 0.08, 0.12,$ and 0.167 (top to bottom). The inset shows the low-temperature behavior. The displayed data have converged in system size. Statistical errors are the width of the line.

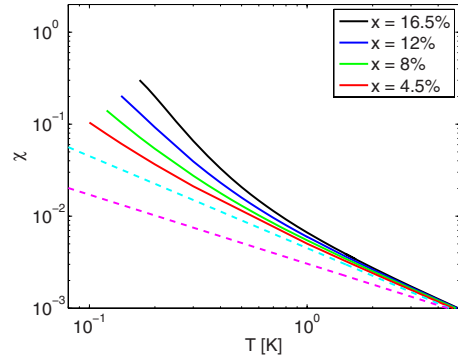


FIG. 5. (Color online) Susceptibility per spin as a function of temperature for $x=0.167, 0.12, 0.08,$ and 0.045 (top to bottom, solid lines). The dashed lines have slope -1 and -0.75 (lower line). Statistical errors are the width of the line and the data have converged in system size.

$x=0.045$ and 0.167 , respectively. Experiments reported in Ref. 2 found that $T_{cw}=0.05$ and 0.16 for $x=0.045$ and 0.167 , respectively. From Fig. 3 we see that while our calculated Curie-Weiss temperature is higher than the mean-field critical temperature, the experimental results are lower. We therefore reach qualitative, but not quantitative, agreement with this set of experiments. However, there is no experimental consensus on the functional form of the susceptibility and a later set of measurements by the same group report a scaling of the form $\chi \sim T^{-0.75}$ for $x=0.045$.⁸ In order to further analyze the functional form we plot our results for the susceptibility in a log-log plot in Fig. 5. From the inserted straight lines we see the Curie scaling $\chi \sim T^\alpha$ with $\alpha=-1$ at higher temperatures. As the temperature is lowered the susceptibility diverges faster, with an exponent $\alpha < -1$, contrary to reported measurements $\alpha=-0.75$.⁸ The experimental data was explained by off-diagonal terms in the dipolar interaction that arise when the material is diluted. Our omission of these terms could explain the discrepancy, but the fact remains that our results agree quite well with the earlier measurements of the susceptibility. Furthermore, the reported scaling of $\chi \sim T^{-0.75}$ persists up to $T=2$ K, and given that the average diagonal local dipolar field is of the order of $1.53 \times 0.045 \approx 0.07$ K it is surprising that there are deviations from Curie scaling at such elevated temperatures. Finally, experimental data for the susceptibility have also been argued to be well modeled by an exponential low-temperature form⁹ $\chi = \exp(-T/T_0)$. Plotting our results for χ in a semilogarithmic plot does not result in a straight line over any significant temperature interval.

In order to compare the various results for the static susceptibility for the high dilution $x=0.045$ we display all the measurements in Fig. 6. We have shifted the curves vertically to display the functional form better. We see that the data from Ref. 8 follow the form $\chi \sim T^{-0.75}$ over the whole temperature range from 0.05 to 2 K. In the high-temperature limit our calculation, as well as data from Refs. 2 and 9, tend to the Curie scaling $\chi \sim T^{-1}$. At low temperature our calculation and data from Ref. 2 diverge faster than T^{-1} while data from Ref. 9 grow significantly more slowly. Due to this discrepancy between different experiments it is difficult to de-

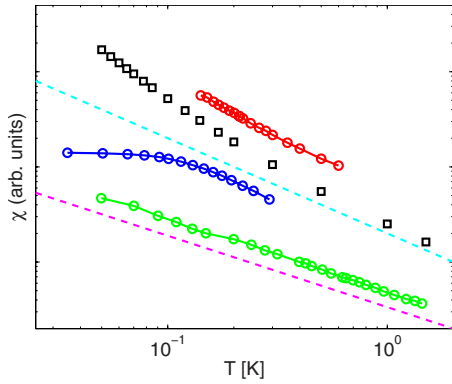


FIG. 6. (Color online) Susceptibility at $x=0.045$. From top to bottom the open symbols are experimental data from Ref. 2, Monte Carlo results, and experimental data from Refs. 9 and 8. The dashed lines have slopes of -1 and -0.75 (lower curve). The curves have been separated vertically. Statistical errors are less than the symbol size

termine how well the classical dipolar Ising model reflects the magnetic behavior of $\text{LiHo}_x\text{Y}_{1-x}\text{F}_4$ in the high-dilution limit. More measurements that could explain the above experimental differences would be necessary in order to draw more definite conclusions.

Next, we consider the magnetization of the dilute model. Using a parallel tempering method we are able to determine the magnetization curves to lower temperature than in a previous study,⁵ as can be seen in Fig. 7. Notice that, for a given dilution, the magnetization increases with system size for intermediate dilution ($x=0.375$), while it decreases in the more dilute systems ($x=0.25$ and $x=0.30$). Extrapolating to the ground state we obtain the ground-state magnetization curve in Fig. 8. Finite-size effects and statistical errors prevent us from a very exact determination, but the curve indicates that the critical concentration x_c , where the magnetization vanishes, is about $x_c=0.24 \pm 0.03$, which is a bit higher than the value $x_c=0.21 \pm 0.02$ reported in a previous

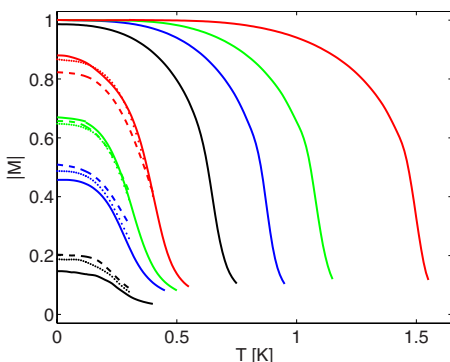


FIG. 7. (Color online) Magnetization per spin as a function of temperature for dilutions $x=0.25, 0.3, 0.33, 0.375, 0.5, 0.625, 0.75$, and 1 (left to right). At low dilution the result is for 10^3 unit cells, while for $x=0.3, 0.33$, and 0.375 the system sizes are 6^3 (dashed line), 8^3 (dotted line), and 10^3 unit cells. For the highest dilution ($x=0.25$) the system sizes are 12^3 (dashed line), 14^3 (dotted line), and 16^3 unit cells. Statistical errors are less than the displayed system size effects.

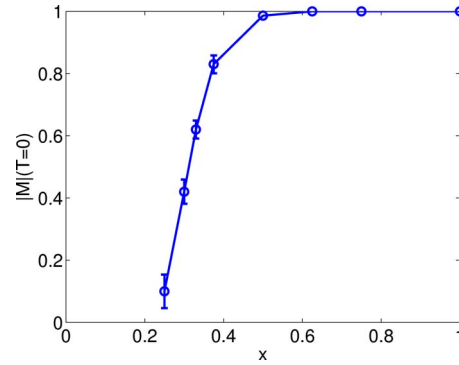


FIG. 8. (Color online) Ground-state magnetization per spin as a function of dilution.

calculation.⁵ We are not aware of any precise experimental determination of x_c , but our result is consistent with experiments that report a spin-glass phase at $x=0.167$ but a ferromagnetic state at $x=0.3$.² Our results also compare well with a previous zero-temperature Monte Carlo study of Ising dipoles on a diluted bcc lattice,²⁴ where it was found that $x_c=0.3 \pm 0.1$.

Finally, we consider the disordered phase for $x < x_c$. We calculate the Binder ratio for the spin overlap, g_q , in the disordered phase. If there is a stable glass phase the curves for different system sizes are expected to cross at the freezing temperature. In a previous study⁵ no crossing was found, indicating that there is no freezing of the spin glass. Here we have repeated the calculation using the parallel tempering method in order to obtain more reliable data in the highly disordered phase, but our results do not differ in any substantial way from those shown in Ref. 5. In order to analyze the nature of the disordered phase further we also consider the spin-glass susceptibility χ_{SG} . In a study of the Heisenberg spin glass it was argued that the Binder ratio of the spin overlap may not intersect at the freezing temperature for all boundary conditions.²⁵ The study suggests that the divergence of the spin-glass susceptibility may be a better indicator of the freezing transition. Since many properties of the long-range dipolar model are quite sensitive to the choice of boundary conditions, we therefore show results for the inverse spin-glass susceptibility in Fig. 9. Experimentally the transition is observed at about $T_g=0.13$ K, yielding $T_g^2=0.017$ K².²⁶ The finite-size effects in Fig. 9 are very small and the spin-glass susceptibility does not appear to diverge at a finite temperature. Since there is quite convincing experimental evidence for a spin-glass transition¹¹ at $x=0.167$, the results are puzzling, and either there are some aspects of the simulations of the glassy dipolar phase that differ from the short-range Ising spin glass or the neglected off-diagonal terms in the Hamiltonian are necessary to stabilize the glassy phase observed in $\text{LiHo}_{0.167}\text{Y}_{0.833}\text{F}_4$. Alternatively there is no freezing of the dipolar glass, as suggested by a different set of experiments.^{9,12}

IV. DISCUSSION AND CONCLUSION

In this work we have made direct comparisons between calculations done on an effective Ising dipolar model and

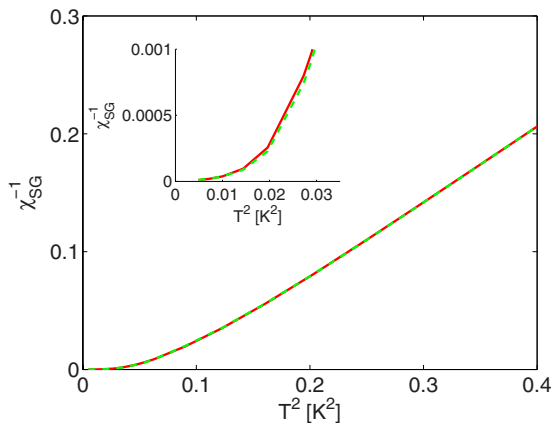


FIG. 9. (Color online) Inverse spin-glass susceptibility at dilution $x=0.167$. Displayed system sizes are 12^3 (dashed line) and 14^3 (solid line) unit cells and statistical errors are smaller than the finite-size effects. In Ref. 2 it is found experimentally that freezing occurs at about $T_g^2=0.017$ K², and the inset shows the behavior at low temperature.

experimental data obtained for $\text{LiHo}_x\text{Y}_{1-x}\text{F}_4$. Obtaining non-perturbative results beyond mean-field theory for the classical dipolar model is an essential step on the way to understanding the physical properties of $\text{LiHo}_x\text{Y}_{1-x}\text{F}_4$. We have focused on the static susceptibility and specific heat. Probably due to the slow dynamics in the highly disordered phase, different sets of experiments do not agree very well. Nevertheless, our calculation agrees well with static susceptibility measurements in Ref. 2, yielding a functional form $\chi \sim 1/(T-T_{\text{cw}})$ in the highly disordered regime. We do not find scaling of the form $\chi \sim T^{-0.75}$ and $\chi \sim \exp(-T/T_0)$

reported in Refs. 8 and 9. Our specific heat displays a broad maximum, in qualitative agreement with recent experiments,¹⁰ but unlike the experiments the position of the maximum scales with the dilution $C_{\text{max}}(T) \sim x$ in our calculation. Our results for the specific heat are not in qualitative agreement with the double peak observed in Ref. 8. Finally, we do not observe a freezing of the spin glass, in agreement with some experiments,^{9,12} while other experiments provide evidence of freezing.^{2,11} The reason for this difference is unclear and deserves further experimental, theoretical, and numerical research.

Some of the difference between our calculation and the experimental results can certainly be explained by quantum-mechanical terms that are not included in our classical model. We have ignored the hyperfine coupling between nuclear and electronic spins. In the low-temperature or high-dilution limit this is generally important, particularly in the presence of an external transverse field. In this study we do not consider an applied magnetic field, and the hyperfine coupling is expected to renormalize the interspin coupling.¹⁷ Including the hyperfine coupling could therefore explain some of the differences between our calculations and the experiments. We have also ignored off-diagonal terms in the dipolar Hamiltonian, which result in an effective random transverse field.^{17,18,27-29} Including these terms in the calculation would be an important next step in interpreting the measurements on $\text{LiHo}_x\text{Y}_{1-x}\text{F}_4$.

ACKNOWLEDGMENTS

We thank M. Gingras and S. Girvin for useful discussions. This work was supported by the Göran Gustafsson Foundation and the Swedish Research Council.

- ¹D. Bitko, T. F. Rosenbaum, and G. Aeppli, Phys. Rev. Lett. **77**, 940 (1996).
- ²D. H. Reich, B. Ellman, J. Yang, T. F. Rosenbaum, G. Aeppli, and D. P. Belanger, Phys. Rev. B **42**, 4631 (1990).
- ³J. Brooke, D. Bitko, T. F. Rosenbaum, and G. Aeppli, Science **284**, 779 (1999).
- ⁴P. B. Chakraborty, P. Henelius, H. Kjønsgberg, A. W. Sandvik, and S. M. Girvin, Phys. Rev. B **70**, 144411 (2004).
- ⁵A. Biltmo and P. Henelius, Phys. Rev. B **76**, 054423 (2007).
- ⁶B. K. Chakrabarti, A. Dutta, and P. Sen, *Quantum Ising Phases and Transitions in Transverse Ising Models* (Springer, New York, 1996).
- ⁷S. Sachdev, *Quantum Phase Transitions* (Cambridge University Press, Cambridge, England, 1999).
- ⁸S. Ghosh, T. F. Rosenbaum, G. Aeppli, and S. N. Coppersmith, Nature (London) **425**, 48 (2003).
- ⁹P. E. Jönsson, R. Mathieu, W. Wernsdorfer, A. Tkachuk, and B. Barbara, Phys. Rev. Lett. **98**, 256403 (2007).
- ¹⁰J. A. Quilliam, C. G. A. Mugford, A. Gomez, S. W. Kycia, and J. B. Kycia, Phys. Rev. Lett. **98**, 037203 (2007).
- ¹¹C. Ancona-Torres, D. M. Silevitch, G. Aeppli, and T. F. Rosenbaum, Phys. Rev. Lett. **101**, 057201 (2008).
- ¹²P. E. Jönsson, R. Mathieu, W. Wernsdorfer, A. Tkachuk, and B. Barbara, arXiv:0803.1357 (unpublished).
- ¹³J. Snider and C. C. Yu, Phys. Rev. B **72**, 214203 (2005).
- ¹⁴S. M. A. Tabei, M. J. P. Gingras, Y. J. Kao, and T. Yavors'kii, arXiv:0801.0443 (to be published).
- ¹⁵M. Schechter and P. C. E. Stamp, Phys. Rev. B **78**, 054438 (2008).
- ¹⁶S. M. A. Tabei, F. Vernay, and M. J. P. Gingras, Phys. Rev. B **77**, 014432 (2008).
- ¹⁷M. Schechter and P. C. E. Stamp, Phys. Rev. Lett. **95**, 267208 (2005).
- ¹⁸S. M. A. Tabei, M. J. P. Gingras, Y.-J. Kao, P. Stasiak, and J.-Y. Fortin, Phys. Rev. Lett. **97**, 237203 (2006).
- ¹⁹P. P. Ewald, Ann. Phys. **369**, 253 (1921).
- ²⁰R. H. Swendsen and J.-S. Wang, Phys. Rev. Lett. **57**, 2607 (1986).
- ²¹D. J. Earl and M. W. Deem, Phys. Chem. Chem. Phys. **7**, 3910 (2005).
- ²²A. Kone and D. A. Kofke, J. Chem. Phys. **122**, 206101 (2005).
- ²³K. Binder and A. P. Young, Rev. Mod. Phys. **58**, 801 (1986).
- ²⁴H. J. Xu, B. Bergersen, F. Niedermayer, and Z. Racz, J. Phys.: Condens. Matter **3**, 4999 (1991).
- ²⁵D. A. Stariolo, Physica A **253**, 1 (1998).

²⁶W. Wu, D. Bitko, T. F. Rosenbaum, and G. Aeppli, Phys. Rev. Lett. **71**, 1919 (1993).

²⁷D. M. Silevitch, D. Bitko, S. Ghosh, G. Aeppli, and T. F. Rosenbaum, Nature (London) **448**, 567 (2007).

²⁸M. Schechter and N. Laflorencie, Phys. Rev. Lett. **97**, 137204 (2006).

²⁹M. Schechter, Phys. Rev. B **77**, 020401(R) (2008).